

Proceeding Paper

# Temperature and Pressure-Induced Phase Transitions in $\text{Cu}_2\text{ZnSnS}_4$ and $\text{Cu}_2\text{ZnGeS}_4$ : Thermodynamic Analysis and Structural Transformations <sup>†</sup>

Mohamed Issam Ziane <sup>1,\*</sup> , Hamza Bennacer <sup>2</sup> and Moufdi Hadjab <sup>2</sup>

<sup>1</sup> Higher School of Electrical and Energetic Engineering of Oran (ESGEEO), Oran 31000, Algeria

<sup>2</sup> Department of Electronics, Faculty of Technology, University of M'sila, M'Sila 28000, Algeria; hz.bennacer@gmail.com (H.B.); moufdi84@yahoo.fr (M.H.)

\* Correspondence: issam1308@yahoo.fr

<sup>†</sup> Presented at the 4th International Electronic Conference on Applied Sciences, 27 October–10 November 2023; Available online: <https://asec2023.sciforum.net/>.

**Abstract:** This study focuses on investigating the phase transitions in two materials,  $\text{Cu}_2\text{ZnSnS}_4$  (CZTS) and  $\text{Cu}_2\text{ZnGeS}_4$  (CZGS), which are important for understanding their structural and functional properties. The temperature and pressure-induced tetragonal-orthorhombic phase transitions in these materials are analyzed using density functional theory (DFT) and the quasi-harmonic Debye model. The research aims to examine the changes in the material's structure and the associated thermodynamic properties during these phase transitions. The results reveal that both compounds exhibit a negative value of  $\delta H_{mix}$ , indicating the release of energy during the mixing process, which suggests an exothermic nature. The DFT calculations at zero temperature and pressure demonstrate that the stannite structure represents the ground state configuration of the  $\text{Cu}_2\text{ZnSnS}_4$  system (with  $x_{Ge} = 0\%$ ), compared to the wurtzite-stannite structure. The calculations also show that the difference in enthalpies of formation ( $\delta H$ ) between the stannite and wurtzite-stannite phases for CZTS is estimated to be 8.884 meV per atom. Regarding  $\text{Cu}_2\text{ZnGeS}_4$ , the wurtzite-stannite structure is found to be the most stable, closely followed by the stannite structure, with enthalpies of formation of  $-4.833 \text{ eV}\cdot\text{atom}^{-1}$  and  $-4.804 \text{ eV}\cdot\text{atom}^{-1}$ , respectively. Notably, there are no definitive reports on enthalpy studies for the  $\text{Cu}_2\text{ZnGeS}_4$  system in the existing literature. Understanding the behavior of these materials under different conditions can contribute to the development of improved performance and stability of devices based on CZTS and CZGS.

**Keywords:** phase transitions;  $\text{Cu}_2\text{ZnSnS}_4$ ;  $\text{Cu}_2\text{ZnGeS}_4$ ; Gibbs energy; stannite; wurtzite-stannite



**Citation:** Ziane, M.I.; Bennacer, H.; Hadjab, M. Temperature and Pressure-Induced Phase Transitions in  $\text{Cu}_2\text{ZnSnS}_4$  and  $\text{Cu}_2\text{ZnGeS}_4$ : Thermodynamic Analysis and Structural Transformations. *Eng. Proc.* **2023**, *56*, 127. <https://doi.org/10.3390/ASEC2023-16639>

Academic Editor: Nunzio Cennamo

Published: 19 December 2023



**Copyright:** © 2023 by the authors. Licensee MDPI, Basel, Switzerland. This article is an open access article distributed under the terms and conditions of the Creative Commons Attribution (CC BY) license (<https://creativecommons.org/licenses/by/4.0/>).

## 1. Introduction

Photovoltaics stands out as a highly promising avenue for achieving a cost-effective alternative energy source, and the research efforts directed towards this domain are consistently on the rise. The materials utilized as the absorber layer in solar cells must meet several key criteria: they should feature an appropriate bandgap, exhibit a notable light absorption coefficient across the solar radiation spectrum, demonstrate enhanced mobility of charge carriers generated by light, incorporate economically viable and eco-friendly components, seamlessly integrate with thin-film deposition methods, and maintain compatibility with the overall fabrication processes.

In the past few years, ternary and quaternary chalcogenides have captured the interest of researchers worldwide. These materials, with their versatile properties, have been extensively studied for numerous applications aimed at enhancing the efficiency of light conversion in devices, improving overall performance, and achieving cost-effectiveness. Quaternary chalcogenide semiconductors are a subgroup of chalcogenide materials that consist of a combination of four elements. Typically, these elements encompass sulfur,

selenium, tellurium, and one or more additional elements derived from groups 3 to 6 of the periodic table.

Quaternary chalcogenides have found significant utility in solar cell technology. Examples such as  $\text{Cu}_2\text{ZnSnS}_4$  and  $\text{Cu}_2\text{ZnGeS}_4$  are renowned for their exceptional capability to efficiently transform sunlight into electrical energy [1–3]. Furthermore, these compounds are constructed from elements that are both environmentally friendly and abundantly available in the Earth's crust. This characteristic holds the potential to decrease the manufacturing expenses associated with solar cells [4]. These materials exhibit various potential phases stemming from rearrangements of their cations. For instance, there are stannite or kesterite-type structures, which are essentially derived from sphalerite unit cells through the organization of metals within cation sites. Additionally, there exist wurtzite-stannite or wurtzite-kesterite structures, which emerge from the wurtzite lattice and conform to the valence octet rule. Each phase can be characterized by its unique geometry. The stannite (I-42m) and kesterite (I-4) structures both exhibit tetragonal symmetry, and the wurtzite-stannite (Pmn21) and wurtzite-kesterite (Pc) structures possess an orthorhombic geometry. Furthermore, an intriguing phase known as the 'disordered kesterite' phase (I-42m) has been identified. In this phase, there is a random distribution of copper and zinc atoms within the 2c and 2d Wyckoff positions [5].

In this study, the objective is to conduct ab initio calculations to investigate the structural and thermodynamic characteristics of the quaternary compounds  $\text{Cu}_2\text{ZnSnS}_4$  and  $\text{Cu}_2\text{ZnGeS}_4$ . Specifically, we will focus on the stannite and wurtzite-stannite structural configurations. To achieve this, we will employ an advanced computational technique rooted in the density functional theory (DFT) framework, utilizing the WIEN2K computational code. Throughout this investigation, we will meticulously compute and analyze lattice parameters, bulk modulus, enthalpy of formation per atom, and various other pertinent thermodynamic properties. The structure of the article is outlined as follows. The Section 2 offers a theoretical outline of the computational approach utilized. Subsequently, the Section 3 will present the findings and engage in corresponding discussions. Lastly, a concise summary of this present research is provided in the Section 4.

## 2. Computational Methods

In this study, we employed first-principles calculations to thoroughly examine the geometry optimization, structural characteristics, and thermodynamic properties of the stannite (St) and wurtzite-stannite (WSt) structures of  $\text{Cu}_2\text{ZnSnS}_4$  (CZTS) and  $\text{Cu}_2\text{ZnGeS}_4$  (CZGS). To achieve this, we employed the full-potential linear-augmented-plane-wave plus local-orbital method within the density functional theory framework, facilitated by the WIEN2K code [6]. For this investigation, we considered conventional cells of CZTS in the form of a 64-atom ( $2 \times 2 \times 2$ ) supercell. Meanwhile, in the case of the wurtzite-stannite (WSt) phase, a ( $1 \times 1 \times 2$ ) supercell was employed. The calculations were conducted utilizing 64-atom supercells for both the stannite (St) and wurtzite-stannite (WSt) phases. The exchange-correlation effects were accounted for using the generalized gradient approximation (GGA), employing the revised Perdew–Burcke–Ernzerhof (PBEsol) parameterization [7]. Throughout the computations, all atomic positions were meticulously relaxed to minimize quantum-mechanical forces.

## 3. Results

As previously mentioned, the structural optimization and relaxation were conducted by adjusting the lattice parameters within a specified unit cell. These adjustments were carried out for various fixed unit cell volumes around the experimentally established ground state volume. The objective was to minimize the total energy of the supercell by varying the volume of the supercell, as well as the  $b/a$  and  $c/a$  parameters. This procedure allowed us to determine the equilibrium lattice parameters accurately. To analyze the relationship between volume and energy, we employed the third-order Murnaghan equation-of-state (EOS) to fit the resulting volume–energy curve. The outcomes of this analysis, including

the optimized lattice parameters (a, b, c), have been compiled in Table 1. In addition, we have included corresponding experimental results from existing literature sources for reference. From the tabulated data, it is apparent that there is a considerable degree of agreement between our computed lattice parameters for  $\text{Cu}_2\text{ZnSnS}_4$  and  $\text{Cu}_2\text{ZnGeS}_4$  and the experimental values found in the literature. This congruence underscores the accuracy of our computational approach and its ability to reliably predict structural properties.

**Table 1.** Optimized lattices parameters (a), (b), and (c), b/a and c/a ratio, and the calculated enthalpies of formation at 0 KT.

Compound	a[Å]	b[Å]	c[Å]	b/a	c/a	$\Delta H$ [eV/atom]
<b><math>\text{Cu}_2\text{ZnSnS}_4</math></b>						
GGAPBEsol[St]	5.383	-	10.767	-	1.999	-4.706
GGAPBEsol[WSt]	7.757	6.475	6.217	0.834	0.801	-4.698
Exp.[St]	5.455 <sup>a</sup>	-	10.880 <sup>a</sup>	-	1.994 <sup>a</sup>	-
Exp.[WSt]	7.973 <sup>b</sup>	6.611 <sup>b</sup>	6.290 <sup>b</sup>	0.829 <sup>b</sup>	0.781 <sup>b</sup>	-
<b><math>\text{Cu}_2\text{ZnGeS}_4</math></b>						
GGAPBEsol[ST]	5.306	-	10.421	-	1.963	-4.804
GGAPBEsol[WSt]	7.435	6.423	6.128	0.863	0.824	-4.833
Exp.[St]	5.346 <sup>c</sup>	-	10.518 <sup>c</sup>	-	1.968 <sup>c</sup>	-
Exp.[WSt]	7.509 <sup>c</sup>	6.479 <sup>c</sup>	6.185 <sup>c</sup>	0.862 <sup>c</sup>	0.824 <sup>c</sup>	-

<sup>a</sup> Ref. [8]; <sup>b</sup> Ref. [9]; <sup>c</sup> Ref. [10].

The enthalpy of formation per atom ( $\Delta_f H$ ) for our materials is determined by subtracting the total energy ( $E_{\text{minCZXS}}$  with  $X = \text{Sn}$  or  $\text{Ge}$ ) of the compound in its equilibrium crystal structure from the sum of energies associated with the constituent elements, considering stoichiometric ratios of Cu, Zn, Sn (or Ge), and S. Our computed ( $\Delta_f H$ ) values, utilizing the GGAPBEsol approximation, are anticipated and showcased in Table 1, following the subsequent expressions [11]:

$$\Delta_f H(\text{Cu}_2\text{ZnXS}_4) = \left[ E_{\text{Cu}_2\text{ZnXS}_4}^{\text{min}} - [2E_{\text{Cu}}^{\text{min}} + E_{\text{Zn}}^{\text{min}} + E_{\text{X}}^{\text{min}} + 4E_{\text{S}}^{\text{min}}] \right] / n \quad (1)$$

where, X is Sn or Ge atoms and  $n$  is the number of atoms in the supercell. As depicted in Table 1, the  $\text{Cu}_2\text{ZnSnS}_4$  compound exhibits the stannite structure as its stable phase, with a preference over the wurtzite-stannite structure. Conversely, for  $\text{Cu}_2\text{ZnGeS}_4$ , the wurtzite-stannite configuration emerges as the most stable structure. The computational results reveal that the difference in enthalpies of formation between the stannite and wurtzite-stannite phases is relatively minimal in CZTS when compared to CZGS. The difference in enthalpies of formation ( $\delta H$ ) between the stannite and wurtzite-stannite phases for CZTS is estimated to be 8.884 meV per atom.

In this research, we employ the quasi-harmonic Debye model code known as GIBBS2, which was developed by Otero-de-la-Roza et al. [12] to forecast thermodynamic properties across a range of temperatures and pressures. Specifically, we utilize the non-equilibrium Gibbs free energy function to investigate the potential occurrence of phase transitions when subjecting the system to different combinations of temperature and pressure.

Examining the plots in Figure 1 reveals that the CZTS compound consistently maintains its stable stannite phase under various applied pressures. On the other hand, for the CZGS compound, the introduction of pressure initiates a phase transition from wurtzite-stannite to stannite at approximately 40 GPa. Additionally, the same figure demonstrates that changes in temperature have no observable impact on the crystal structures of both materials; they remain unaffected regardless of the temperature variations.

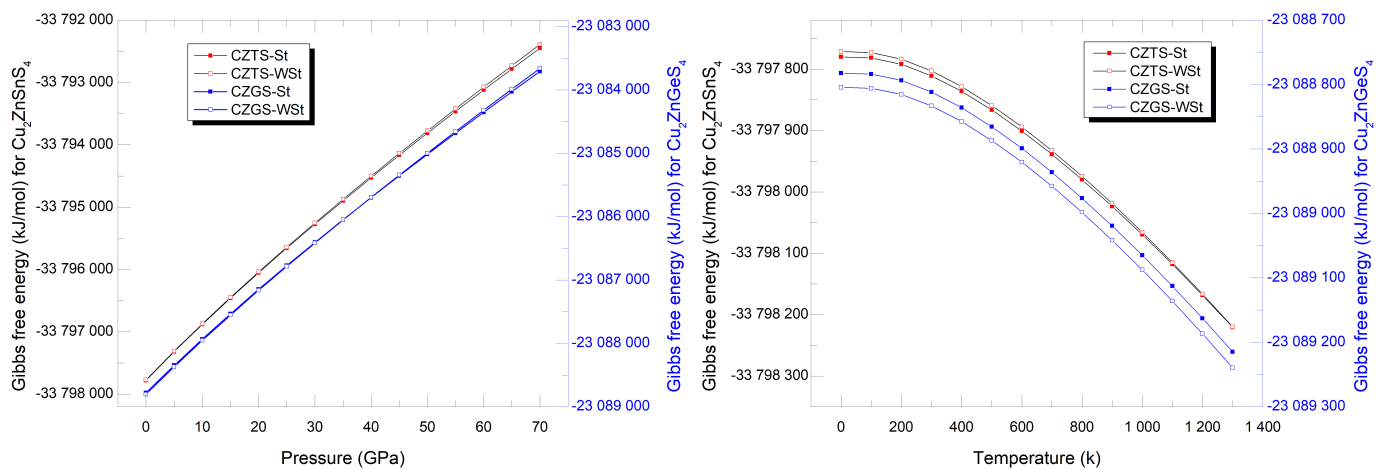


**Figure 1.** Influence of pressure and temperature on the Gibbs free energy in CZTS and CZGS compounds.

#### 4. Conclusions

The structural and thermodynamic characteristics of  $\text{Cu}_2\text{ZnSnS}_4$  and  $\text{Cu}_2\text{ZnGeS}_4$  under varying temperature and pressure conditions were thoroughly examined through the utilization of DFT calculations in conjunction with the quasi-harmonic Debye model. When germanium is substituted with tin, a common outcome is a reduction in the lattice parameters due to the smaller size of germanium atoms. Additionally, it was found that the mixing enthalpy is negative (indicating an exothermic process) for the stannite-based structure, indicating that the formation of the alloy is thermodynamically favorable.

Through an analysis of the Gibbs energy variations, we gained valuable insights into the thermodynamic behavior and the conformational and structural transitions that these alloys experience under different temperature conditions. Furthermore, our thermodynamic and phase analyses, based on Gibbs calculations, unveiled a noteworthy microstructural evolution in the  $\text{Cu}_2\text{ZnGeS}_4$  compound. As pressure increases, this compound undergoes a transition from the orthorhombic wurtzite-stannite phase to the tetragonal stannite phase. In contrast,  $\text{Cu}_2\text{ZnSnS}_4$  maintains its tetragonal structure consistently throughout the study.

**Author Contributions:** Writing—review and editing, M.I.Z.; formal analysis, H.B. and M.H. All authors have read and agreed to the published version of the manuscript.

**Funding:** This research received no external funding.

**Institutional Review Board Statement:** Not applicable.

**Informed Consent Statement:** Not applicable.

**Data Availability Statement:** Data sharing does not apply to this work.

**Conflicts of Interest:** The authors declare no conflicts of interest.

#### References

1. Tajima, S.; Umehara, M.; Hasegawa, M.; Mise, T.; Itoh, T.  $\text{Cu}_2\text{ZnSnS}_4$  photovoltaic cell with improved efficiency fabricated by high temperature annealing after CdS buffer-layer deposition. *Prog. Photo. Res. Appl.* **2017**, *25*, 14–22. [[CrossRef](#)]
2. Ziane, M.I.; Bennacer, H.; Mostefaoui, M.; Tablaoui, M.; Hadjab, M.; Saim, A.; Bekhedda, K. Anisotropic optical properties of  $\text{Cu}_2\text{ZnSn}(\text{S}_x\text{Se}_{1-x})_4$  solid solutions: First-principles calculations with TB-mBJ+U. *Optik* **2021**, *243*, 167490. [[CrossRef](#)]
3. Karthik, M.; Abhinav, J.; Shankar, K.V. Morphological and Mechanical Behaviour of Cu–Sn Alloys—A review. *Met. Mater. Int.* **2021**, *27*, 1915–1946. [[CrossRef](#)]
4. Sanchez, M.F.; Sanchez, T.G.; Courel, M.; Reyes-Vallejo, O.; Sanchez, Y.; Saucedo, E.; Sebastian, P.J. Effect of post annealing thermal heating on  $\text{Cu}_2\text{ZnSnS}_4$  solar cells processed by sputtering technique. *Sol. Energy* **2022**, *237*, 196–202. [[CrossRef](#)]
5. Khelfane, A.; Ziane, M.I.; Tablaoui, M.; Hecini, M.; Ouadjaout, D.; Derbal, M. Composition dependence of the optical band gap and the secondary phases via zinc content in CZTS material. *Inorg. Chem. Commun.* **2023**, *151*, 110639. [[CrossRef](#)]
6. Schwarz, K.; Blaha, P. Solid state calculations using WIEN2k. *Comput. Mater. Sci.* **2003**, *28*, 259. [[CrossRef](#)]

7. Perdew, J.P.; Ruzsinszky, A.; Csonka, G.I.; Vydrov, O.A.; Scuseria, G.E.; Constantin, L.A.; Zhou, X.; Burke, K. Constantin, Xiaolan Zhou, and Kieron Burke, Restoring the Density-Gradient Expansion for Exchange in Solids and Surfaces. *Phys. Rev. Lett.* **2008**, *100*, 136406. [[CrossRef](#)] [[PubMed](#)]
8. Nagaoka, A.; Yoshino, K.; Aoyagi, K.; Minemoto, T.; Nose, Y.; Taniyama, T.; Kakimoto, K.; Miyake, H. Thermo physical properties of  $\text{Cu}_2\text{ZnSnS}_4$  single crystal. *J. Cryst. Growth* **2014**, *393*, 167–170. [[CrossRef](#)]
9. Zhao, Y.; Li, D.; Liu, Z. Phase Transitions and Electronic Properties for Zincblende-Derived and Wurtzite-Derived Stannite  $\text{Cu}_2\text{ZnSnS}_4$  Under Pressure. *J. Electron. Mater.* **2017**, *48*, 2812–2821. [[CrossRef](#)]
10. Doverspike, K.; Kershaw, R.; Dwight, K.; Mold, A. Preparation and properties of the system  $\text{Cu}_2\text{Zn}_{1-x}\text{Fe}_x\text{GeS}_4$ . *Mat. Res. Bull.* **1988**, *23*, 959–964. [[CrossRef](#)]
11. Ziane, M.I.; Ouadjaout, D.; Tablaoui, M.; Nouri, R.; Zermane, W.; Djelloul, A.; Bennacer, H.; Mokrani, A.; Hadjab, M.; Abid, H. First-Principle Computed Structural and Thermodynamic Properties of  $\text{Cu}_2\text{ZnSn}(\text{S}_x\text{Se}_{1-x})_4$  Pentanary Solid Solution. *J. Electron. Mater.* **2019**, *48*, 11. [[CrossRef](#)]
12. Otero-de-la-Roza, A.; Abbasi-Pérez, D.; Luaña, V. Gibbs2: A new version of the quasiharmonic model code. II. Models for solid-state thermodynamics, features and implementation. *Comput. Phys. Commun.* **2011**, *10*, 2232–2248. [[CrossRef](#)]

**Disclaimer/Publisher’s Note:** The statements, opinions and data contained in all publications are solely those of the individual author(s) and contributor(s) and not of MDPI and/or the editor(s). MDPI and/or the editor(s) disclaim responsibility for any injury to people or property resulting from any ideas, methods, instructions or products referred to in the content.